

Contents

1	Stability of equilibrium points & bifurcations	3
1.1	Simple population model	3
1.2	Gene control model	3
2	Imperfect bifurcations	6
3	Study of a predator-prey model	9
3.1	A qualitative study for $d = 0$	10
3.2	Bifurcation analysis	15
4	Aero-elastic galloping	18
5	Chaos	21
5.1	Lyapunov exponents of the Lorenz equations	21
5.2	Hindmarsh-Rose neuron model	22
5.3	Chua's circuit	22

4 Aero-elastic galloping

Applying Newton's second law to the bridge element, and introducing $x = \dot{y}$ as its linear velocity, its dynamic behaviour can be described by

$$\begin{aligned}\dot{x} &= 0.5 V^2 C(x/V) - x - 100y \\ \dot{y} &= x\end{aligned}$$

where the constants have been substituted in, and with $C(\alpha) \approx 10^{-2} \alpha - 10^{-3} \alpha^3 + 10^{-5} \alpha^5 - 10^{-8} \alpha^7$ (exact coefficients as in the assignment).

The system has a fixed point at the origin. [Figure 15](#) shows the eigenvalues of the Jacobian at this fixed point, for varying wind speeds V . In low-wind conditions, the system starts out stable, with both eigenvalues having negative real parts (but having nonzero imaginary parts, predicting oscillatory behaviour). At $V = V_C = 42.5985\dots$, the eigenvalues cross the imaginary axis, and the origin transitions from a stable spiral, through a center, to an unstable spiral. V_C is the solution to $\tau = 0$, with $\tau = V A_1/2 - 1$ the trace of the Jacobian at the origin. For very large $V = V_R = 894.6\dots$, the eigenvalues land on the real axis, and the unstable spiral transitions to a repelling star and a repelling node. V_R is the solution to $4\Delta = \tau^2$, with $\Delta = 100$ the determinant of the Jacobian at the origin (see [chapter 3](#)). [Table 2](#) summarises this classification of the origin's stability.

When the nonlinear terms of $C(\alpha)$ are not neglected, $\dot{x}(x)$ will look 'bumpy'. A slight displacement y will shift this bumpy function, so that $\dot{x}(x)$ crosses the x -axis more than once. In one-dimensional systems, this tends to result in fixed points away from the origin. This might then correspond to a limit cycle in the current two-dimensional system. When V then passes the bifurcation V_C , the origin is unstable, and even the tiniest displacement from the origin will end up on the limit cycle. When the model is simulated ([fig. 16](#)), this is indeed what we observe.

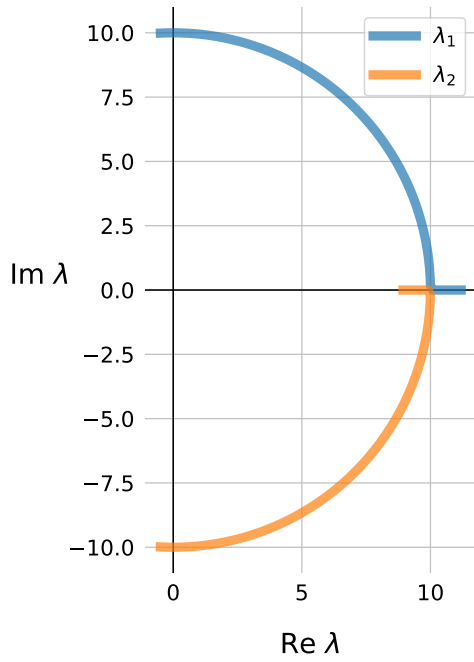


Figure 15: **Linear stability analysis of the bridge model.** Eigenvalues of the Jacobian at the fixed point $(0, 0)$, for $V \in [0, 900]$ ($V = 0$ in the left half plane, at $\text{Re } \lambda_i = -0.5$).

Wind speed V	Stability of origin
$V < V_C$	Stable spiral
$V = V_C$	Center
$V_C < V < V_R$	Unstable spiral
$V = V_R$	Repelling star
$V > V_R$	Repelling node

Table 2: **Classification of the fixed point.** $V_C \approx 42.6$ and $V_R \approx 895$.

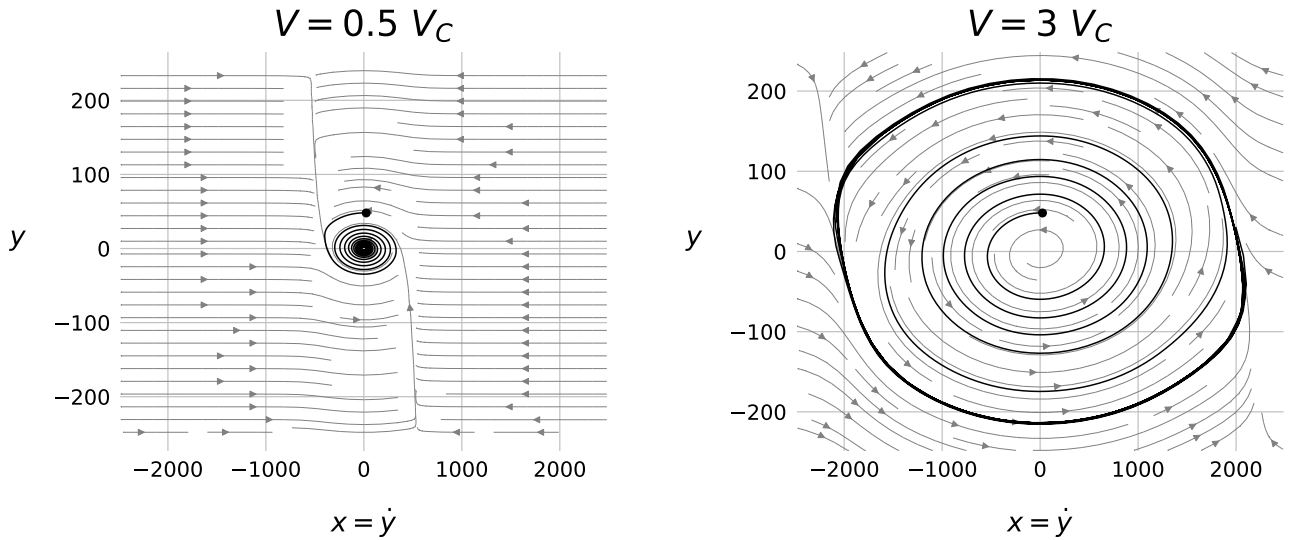


Figure 16: **Phase space diagrams of the bridge model.** *Left:* below the critical wind speed V_C , displacements return to the origin. *Right:* above the critical wind speed, the same starting phase point will end up on a limit cycle.

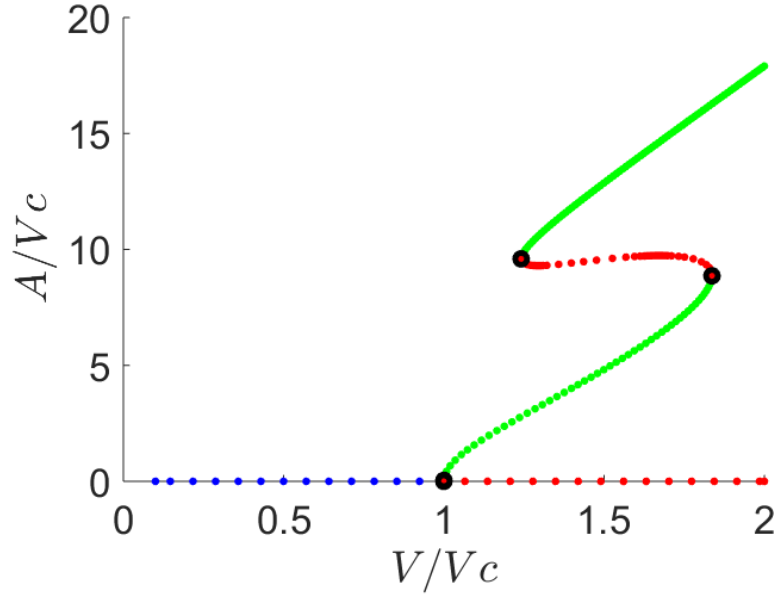


Figure 17: **Aero-elastic galloping bifurcation diagram.** A is the maximal displacement during the limit cycle. Blue and green dots indicate stable fixed points and stable limit cycles, respectively. Red dots indicate unstable fixed points and unstable limit cycles. Black circles mark saddle-node bifurcations.

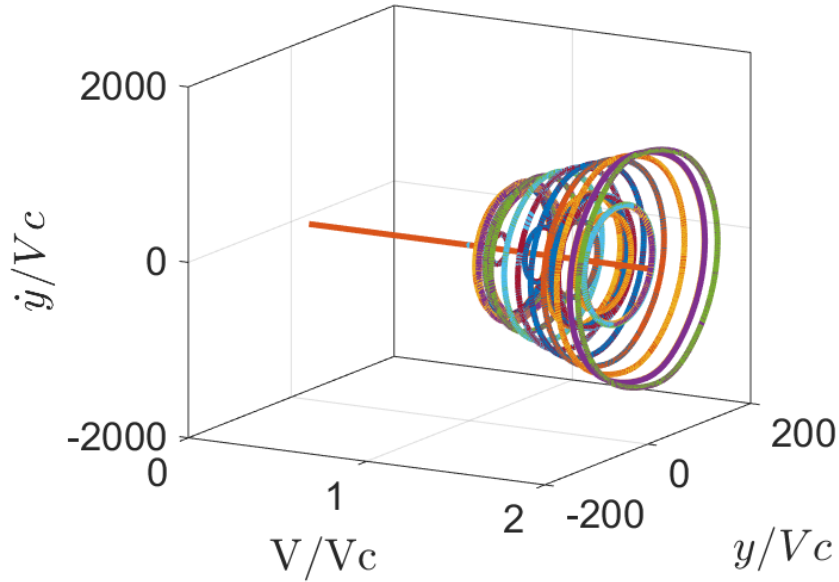


Figure 18: **Phase space orbits.** Orbits (y, \dot{y}) for different wind speeds V . Note the inner manifold, indicative of hysteresis behaviour.